

Neural Network Verification with Branch-and-Bound for General Nonlinearities

Zhouxing Shi^{*1}, Qirui Jin^{*2}, Zico Kolter³, Suman Jana⁴, Cho-Jui Hsieh¹, Huan Zhang⁵

¹University of California, Los Angeles ²University of Michigan

³Carnegie Mellon University ⁴Columbia University ⁵University of Illinois Urbana-Champaign

z.shi@ucla.edu, qiruijin@umich.edu

zkolter@cs.cmu.edu, suman@cs.columbia.edu, chohsieh@cs.ucla.edu, huan@huan-zhang.com

**Equal contribution*

Abstract

Branch-and-bound (BaB) is among the most effective methods for neural network (NN) verification. However, existing works on BaB have mostly focused on NNs with piecewise linear activations, especially ReLU networks. In this paper, we develop a general framework, named GenBaB, to conduct BaB for general nonlinearities in general computational graphs based on linear bound propagation. To decide which neuron to branch, we design a new branching heuristic which leverages linear bounds as shortcuts to efficiently estimate the potential improvement after branching. To decide nontrivial branching points for general nonlinear functions, we propose to optimize branching points offline, which can be efficiently leveraged during verification with a lookup table. We demonstrate the effectiveness of our GenBaB on verifying a wide range of NNs, including networks with activation functions such as Sigmoid, Tanh, Sine and GeLU, as well as networks involving multi-dimensional nonlinear operations such as multiplications in LSTMs and Vision Transformers. Our framework also allows the verification of general nonlinear computation graphs and enables verification applications beyond simple neural networks, particularly for AC Optimal Power Flow (ACOPF). GenBaB is part of the latest α, β -CROWN, the winner of the 4th International Verification of Neural Networks Competition (VNN-COMP 2023).

1 Introduction

Neural network (NN) verification aims to formally verify whether a neural network satisfies specific properties, such as safety or robustness, prior to its deployment in safety-critical applications. Verifiers typically compute certified bounds on the output neurons within a pre-defined input region. As computing exact bounds is NP-complete (Katz et al., 2017) even for simple ReLU networks, it becomes crucial to relax the bound computation process to improve the efficiency. Bound propagation methods (Wang et al., 2018b; Wong & Kolter, 2018; Zhang et al., 2018; Dvijotham et al., 2018; Henriksen & Lomuscio, 2020; Singh et al., 2019b) are commonly used, which relax nonlinearities in neural networks into linear lower and upper bounds which can be efficiently propagated.

To obtain tighter verified bounds, Branch-and-Bound (BaB) has been widely utilized (Bunel et al., 2018, 2020; Xu et al., 2021; Lu & Mudigonda, 2020; De Palma et al., 2021; Wang et al., 2021; Ferrari et al., 2021). However, previous works mostly focused on ReLU networks due to the simplicity of ReLU from its piecewise linear nature. Branching a ReLU neuron only requires branching at 0, and it immediately becomes linear in either branch around 0. Conversely, handling neural networks with nonlinearities beyond ReLU introduces additional complexity as the convenience of piecewise linearity diminishes. It is important for verifying many models with non-ReLU nonlinearities, including NNs with non-ReLU activation functions, NNs such as LSTMs (Hochreiter & Schmidhuber, 1997) and Transformers (Vaswani et al., 2017) which have nonlinearities beyond activation functions including multiplication and division, verification applications such as AC Optimal Power Flow (ACOPF) (Guha et al., 2019) where the verification problem is defined on a computational graph consisting of a neural network and also various nonlinear operators encoding the nonlinear constraints to be verified. Although some previous works have considered BaB for NNs beyond ReLU networks, e.g., Henriksen & Lomuscio (2020); Wu et al. (2022) considered BaB on networks with S-shaped activations such as Sigmoid, these works still often specialize in specific and relatively simple types of nonlinearities. A more principled framework for handling general nonlinearities is lacking, leaving ample room for further advancements in verifying non-ReLU networks.

In this paper, we propose **GenBaB**, a principled neural network verification framework with BaB for general nonlinearities. To enable BaB for general nonlinearities beyond ReLU, we first formulate a general BaB framework, and we introduce general branching points, where we may branch at points other than 0 for nonlinear functions, which is needed when the nonlinearity is not simply piecewise linear around 0. We then propose a new branching heuristic named “Bound Propagation with Shortcuts (BBPS)” for branching general nonlinearities, which carefully leverages the linear bounds from bound propagation as shortcuts to efficiently and effectively estimate the bound improvement from branching a neuron. Moreover, we propose to decide nontrivial branching points by pre-optimizing branching points offline, according to the tightness of the resulted linear relaxation for each possibility of pre-activation bounds, and we save the optimized branching points into a lookup table to be efficiently used when verifying an entire NN.

We demonstrate the effectiveness of our GenBaB on a variety of networks, including feedforward networks with Sigmoid, Tanh, Sine, or GeLU activations, as well as LSTMs and Vision Transformers (ViTs). These models involve various nonlinearities including S-shaped activations, periodic trigonometric functions, and also multiplication and division which are multi-dimensional nonlinear operations beyond activation functions. We also enable verification on models for the AC Optimal Power Flow (ACOPF) application (Guha et al., 2019). GenBaB is generally effective and outperforms existing baselines. The improvement from GenBaB is particularly significant for models involving functions with stronger nonlinearity. For example, on a 4×100 network with the Sine activation, GenBaB improves the verification from 4% to 60% instances verified (NNs with the Sine activation have been proposed for neural representations and neural rendering in Sitzmann et al. (2020)).

GenBaB has been integrated to the latest version of α, β -CROWN¹ which is the winner of the 4th International Verification of Neural Networks Competition (VNN-COMP 2023). Code for reproducing the results is available at <https://github.com/shizhouxing/GenBaB>.

2 Background

The NN verification problem. Let $f : \mathbb{R}^d \mapsto \mathbb{R}^K$ be a neural network taking input $\mathbf{x} \in \mathbb{R}^d$ and outputting $f(\mathbf{x}) \in \mathbb{R}^K$. Suppose \mathcal{C} is the input region to be verified, and $s : \mathbb{R}^K \mapsto \mathbb{R}$ is an output specification function, $h : \mathbb{R}^d \mapsto \mathbb{R}$ is the function that combines the NN and the output specification as $h(\mathbf{x}) = s(f(\mathbf{x}))$. NN verification can typically be formulated as verifying if $h(\mathbf{x}) > 0, \forall \mathbf{x} \in \mathcal{C}$ provably holds. A commonly adopted special case is robustness verification given a small input region, where $f(\mathbf{x})$ is a K -way classifier and $h(\mathbf{x}) := \min_{i \neq c} \{f_c(\mathbf{x}) - f_i(\mathbf{x})\}$ checks the worst-case margin between the ground-truth class c and any other class i . The input region is often taken as a small ℓ_∞ -ball with radius ϵ around a data point \mathbf{x}_0 , i.e., $\mathcal{C} := \{\mathbf{x} \mid \|\mathbf{x} - \mathbf{x}_0\|_\infty \leq \epsilon\}$. This is a succinct and useful problem for provably verifying the robustness properties of a model and also for benchmarking NN verifiers, although there are other NN verification problems beyond robustness (Brix et al., 2023). We mainly focus on this setting for its simplicity following prior works.

Linear bound propagation. We develop our GenBaB based on linear bound propagation (Zhang et al., 2018; Xu et al., 2020) for computing the verified bounds of each domain during the BaB. Linear bound propagation can lower bound $h(\mathbf{x})$ by propagating linear bounds w.r.t. the output of one or more intermediate layers as $h(\mathbf{x}) \geq \sum_i \mathbf{A}_i \hat{\mathbf{x}}_i + \mathbf{c}$, where $\hat{\mathbf{x}}_i$ ($i \leq n$) is the output of intermediate layer i in the network with n layers, \mathbf{A}_i are the coefficients w.r.t. layer i , and \mathbf{c} is a bias term. In the beginning, the linear bound is simply $h(\mathbf{x}) \geq \mathbf{I} \cdot h(\mathbf{x}) + \mathbf{0}$ which is actually an equality. In the bound propagation, $\mathbf{A}_i \hat{\mathbf{x}}_i$ is recursively substituted by the linear bound of $\hat{\mathbf{x}}_i$ w.r.t its input. For simplicity, suppose layer $i - 1$ is the input to layer i and $\hat{\mathbf{x}}_i = h_i(\hat{\mathbf{x}}_{i-1})$, where $h_i(\cdot)$ is the computation for layer i . And suppose we have the linear bounds of $\hat{\mathbf{x}}_i$ w.r.t its input $\hat{\mathbf{x}}_{i-1}$ as:

$$\underline{\mathbf{a}}_i \hat{\mathbf{x}}_{i-1} + \underline{\mathbf{b}}_i \leq \hat{\mathbf{x}}_i = h_i(\hat{\mathbf{x}}_{i-1}) \leq \bar{\mathbf{a}}_i \hat{\mathbf{x}}_{i-1} + \bar{\mathbf{b}}_i, \quad (1)$$

with parameters $\underline{\mathbf{a}}_i, \underline{\mathbf{b}}_i, \bar{\mathbf{a}}_i, \bar{\mathbf{b}}_i$ for the linear bounds, and “ \leq ” holds elementwise. Then $\mathbf{A}_i \hat{\mathbf{x}}_i$ can be substituted and lower bounded by $\mathbf{A}_i \hat{\mathbf{x}}_i \geq \mathbf{A}_{i-1} \hat{\mathbf{x}}_{i-1} + (\mathbf{A}_{i,+} \underline{\mathbf{b}}_i + \mathbf{A}_{i,-} \bar{\mathbf{b}}_i)$, where $\mathbf{A}_{i-1} = \mathbf{A}_{i,+} \underline{\mathbf{a}}_i + \mathbf{A}_{i,-} \bar{\mathbf{a}}_i$, (“+” and “-” in the subscripts denote taking positive and negative elements, respectively). In this way the linear bounds are propagated from layer i to layer $i - 1$. Ultimately, the linear bounds can be propagated to the input of the network \mathbf{x} as $h(\mathbf{x}) \geq \mathbf{A}_0 \mathbf{x} + \mathbf{c}$ ($\mathbf{A}_0 \in \mathbb{R}^{1 \times d}$), where the input can be viewed as the 0-th layer. Depending on \mathcal{C} , this linear bound can be concretized into a lower bound without \mathbf{x} . If \mathcal{C} is an ℓ_∞ ball, we have

$$\forall \|\mathbf{x} - \mathbf{x}_0\|_\infty \leq \epsilon, \quad \mathbf{A}_0 \mathbf{x} + \mathbf{c} \geq \mathbf{A}_0 \mathbf{x}_0 - \epsilon \|\mathbf{A}_0\|_1 + \mathbf{c}. \quad (2)$$

To obtain Eq. (1), if h_i is a linear operator, we simply have $\underline{\mathbf{a}}_i \hat{\mathbf{x}}_{i-1} + \underline{\mathbf{b}}_i = \bar{\mathbf{a}}_i \hat{\mathbf{x}}_{i-1} + \bar{\mathbf{b}}_i = h_i(\hat{\mathbf{x}}_{i-1})$ which is h_i itself. Otherwise, linear relaxation is used, which relaxes a nonlinearity and bound the nonlinearity by linear functions. An

¹<https://github.com/Verified-Intelligence/alpha-beta-CROWN>

intermediate bound on $\hat{\mathbf{x}}_{i-1}$ as $\mathbf{l}_{i-1} \leq \hat{\mathbf{x}}_{i-1} \leq \mathbf{u}_{i-1}$ is usually required for the relaxation, which can be obtained by running additional bound propagation and treating the intermediate layers as the output of a network.

3 Method

3.1 Overall Framework

Notations. Although in Section 2, we considered a feedforward NN for simplicity, linear bound propagation has been generalized to general computational graphs (Xu et al., 2020). In our method, we also consider a general computational graph $h(\mathbf{x})$ for input region $\mathbf{x} \in \mathcal{C}$. Instead of a feedforward network with n layers in Section 2, we consider a computational graph with n nodes, where each node i computes some function $h_i(\cdot)$ which may either correspond to a linear layer in the NN or a nonlinearity. We use $\hat{\mathbf{x}}_i$ to denote the output of node i , which may contain many neurons, and we use $\hat{\mathbf{x}}_{i,j}$ to denote the output of the j -th neuron in node i . Intermediate bounds of node i may be needed to relax and bound $h_i(\cdot)$, and we use $\mathbf{l}_{i,j}, \mathbf{u}_{i,j}$ to denote the intermediate lower and upper bound respectively. We use \mathbf{l} and \mathbf{u} to denote all the intermediate lower bounds and upper bounds, respectively, for the entire computational graph.

Overview of GenBaB. In our GenBaB, we branch the intermediate bounds of neurons connected to general nonlinearities. We maintain a dynamic pool of intermediate bound domains, $\mathcal{D} = \{(\mathbf{l}^{(i)}, \mathbf{u}^{(i)})\}_{i=1}^m$, where $m = |\mathcal{D}|$ is the number of current domains, and initially we have $\mathcal{D} = \{(\mathbf{l}, \mathbf{u})\}$ with the intermediate bounds from the initial verification before BaB. Then in each iteration of our BaB, we pop a domain from \mathcal{D} , and we select a neuron to branch and a branching point on its intermediate bounds. To support general nonlinearities, we formulate a new and general branching framework in Section 3.2, where we introduce general branching points, in contrast to branching ReLU activations at 0 only, and we also support more complicated networks architectures where a nonlinearity can involve multiple input nodes or output nodes. In order to decide which neuron we choose to branch, we propose a branching heuristic in Section 3.3 to estimate the potential improvement for each choice of a branched neuron, where we carefully leverage linear bounds as an efficient shortcut for a more precise estimation. Finally, to decide nontrivial branching points, in Section 3.4, we propose to pre-optimize the branching points offline, which aims to produce the tightest linear relaxation after taking the optimized branching point.

Each branching step generates new subdomains. For the new subdomains, we update \mathbf{l}, \mathbf{u} for the branched neurons according to the branching points, and the branching decision is also encoded into the bound propagation as additional constraints by Lagrange multipliers following Wang et al. (2021). For each new subdomain, given updated \mathbf{l}, \mathbf{u} , we use $V(h, \mathcal{C}, \mathbf{l}, \mathbf{u})$ to denote a new verified bound computed with new intermediate bounds \mathbf{l}, \mathbf{u} . Subdomains with $V(h, \mathcal{C}, \mathbf{l}, \mathbf{u}) > 0$ are verified and discarded, otherwise they are added to \mathcal{D} for further branching. We repeat the process until no domain is left in \mathcal{D} and the verification succeeds, or when the timeout is reached and the verification fails.

3.2 Branching for General Nonlinearities

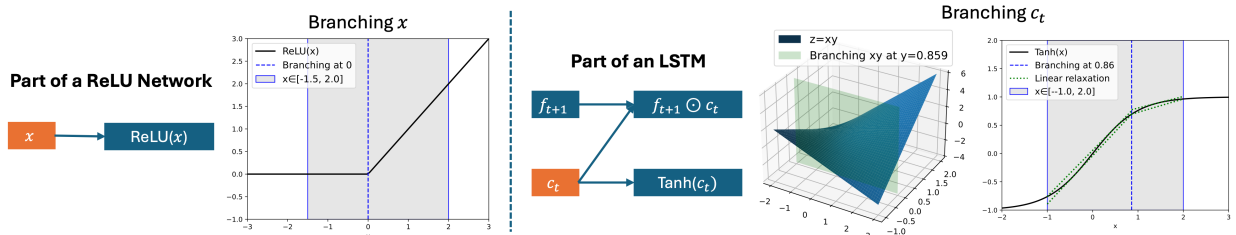


Figure 1: Illustration of the more complicated nature of branching for general nonlinearities (branching a ReLU activation v.s. branching for nonlinearities in an LSTM). Notations for part of an LSTM follows PyTorch’s documentation (<https://pytorch.org/docs/stable/generated/torch.nn.LSTM.html>). Nodes in orange are being branched. For general nonlinearities, branching points can be non-zero (0.86 in the LSTM example here), a nonlinearity can take multiple input nodes ($f_{t+1} \odot c_t$ here), and a node can also be followed by multiple nonlinearities (c_t is followed by a multiplication and also Tanh, and branching c_t affects both two nonlinearities).

As illustrated in Figure 1, branching for general nonlinearities on general computational graphs is more complicated, in contrast to BaB for ReLU networks where it always branches at 0 and ReLU is linear on both sides. For general nonlinearities, we need to consider branching at points other than 0. In addition, unlike typical activation functions, some nonlinearities may take more than one inputs and thereby have multiple input nodes that can be branched, such as

multiplication in LSTM (“ $f_{t+1} \odot c_t$ ” in Figure 1) or Transformers (Hochreiter & Schmidhuber, 1997; Vaswani et al., 2017). On general computational graphs, a node can also be followed by multiple nonlinearities, as appeared in LSTMs (such as “ c_t ” in Figure 1), and then branching the intermediate bounds of this node can affect multiple nonlinearities.

To resolve these challenges, we propose a more general formulation for branching on general computational graphs with general nonlinearities. Each time we consider branching the intermediate bounds of a neuron j in a node i , namely $[l_{i,j}, u_{i,j}]$, if node i is the input of some nonlinearity. We consider branching the concerned neuron into 2 branches with a nontrivial branching point $\mathbf{p}_{i,j}$, as $[l_{i,j}, u_{i,j}] \rightarrow [l_{i,j}, \mathbf{p}_{i,j}], [\mathbf{p}_{i,j}, u_{i,j}]$. Here we consider each node i which is the input to at least one nonlinearity and decide if we branch the intermediate bounds $[l_i, u_i]$ of this node, instead of considering each nonlinearity. This formulation allows us to support nonlinearities with multiple input nodes as well as multiple nonlinearities sharing the input node. In the next two subsections, we will further discuss supporting general computational graphs in our branching heuristic and branching points.

3.3 Which Neuron to Branch? A New Branching Heuristic

We propose a new branching heuristic which is a scoring function for efficiently estimating the new verified bound after branching at a neuron with a branching point, so that we can choose a neuron to branch which potentially lead to a good improvement after the branching. Specifically, we design a function $\tilde{V}(\mathbf{l}, \mathbf{u}, i, j, k, \mathbf{p}_{i,j})$ which estimates the new bound of the k -th ($1 \leq k \leq 2$) branch, after branching neuron j in node i using branching points $\mathbf{p}_{i,j}$. We use $B(\mathbf{l}, \mathbf{u}, i, j, k, \mathbf{p}_{i,j})$ to denote the updated intermediate bounds after this branching, and essentially we aim to use $\tilde{V}(\mathbf{l}, \mathbf{u}, i, j, k, \mathbf{p}_{i,j})$ to efficiently estimate $V(h, \mathcal{C}, B(\mathbf{l}, \mathbf{u}, i, j, k, \mathbf{p}_{i,j}))$ which is the actual verified bound after the branching, but it is too costly to directly compute an actual verified bound for each branching option.

Suppose we consider branching a neuron j in node i and we aim to estimate $V(\cdot)$ for each branch k . In the linear bound propagation, when the bounds are propagated to node i , we have:

$$h(\mathbf{x}) \geq \mathbf{A}_{i,j}^{(k)} \hat{\mathbf{x}}_{i,j} + \mathbf{c}^{(k)} \geq V(h, \mathcal{C}, B(\mathbf{l}, \mathbf{u}, i, j, k, \mathbf{p}_{i,j})), \quad (3)$$

where we use $\mathbf{A}_{i,j}^{(k)}$ and $\mathbf{c}^{(k)}$ to denote the parameters in the linear bounds for the k -th branch. Since we do not update the intermediate bounds except for the branched neurons during BaB for efficiency following Wang et al. (2021), branching a neuron in node i only affects the linear relaxation of nonlinear nodes immediately after node i (i.e., output nodes of i). Therefore, $\mathbf{A}_{i,j}^{(k)}$ and $\mathbf{c}^{(k)}$ can be computed by only propagating the linear bounds from the output nodes of i , using previously stored linear bounds, rather than from the final output of $h(\mathbf{x})$.

For a more efficient estimation, instead of propagating the linear bounds towards the input of the network step by step, we propose a new branching heuristic named Bound Propagation with Shortcuts (BBPS), where we use a shortcut to directly propagate the bounds to the input. Specifically, we save the linear bounds of all the potentially branched intermediate layers during the initial verification before BaB. For every neuron j in intermediate node i , we record:

$$\forall \mathbf{x} \in \mathcal{C}, \quad \hat{\mathbf{A}}_{i,j} \mathbf{x} + \hat{\mathbf{c}}_{i,j} \leq \hat{\mathbf{x}}_{i,j} \leq \bar{\mathbf{A}}_{i,j} \mathbf{x} + \bar{\mathbf{c}}_{i,j}, \quad (4)$$

where $\hat{\mathbf{A}}_{i,j}, \hat{\mathbf{c}}_{i,j}, \bar{\mathbf{A}}_{i,j}, \bar{\mathbf{c}}_{i,j}$ are parameters for the linear bounds. These are obtained when linear bound propagation is used for computing the intermediate bounds $[l_{i,j}, u_{i,j}]$ and the linear bounds are propagated to the input \mathbf{x} . We then use Eq. (4) to compute a lower bound for $\mathbf{A}_{i,j}^{(k)} \hat{\mathbf{x}}_{i,j} + \mathbf{c}^{(k)}$:

$$\mathbf{A}_{i,j}^{(k)} \hat{\mathbf{x}}_{i,j} + \mathbf{c}^{(k)} \geq (\mathbf{A}_{i,j,+}^{(k)} \hat{\mathbf{A}}_{i,j} + \mathbf{A}_{i,j,-}^{(k)} \bar{\mathbf{A}}_{i,j}) \mathbf{x} + \mathbf{A}_{i,j,+}^{(k)} \hat{\mathbf{c}}_{i,j} + \mathbf{A}_{i,j,-}^{(k)} \bar{\mathbf{c}}_{i,j} + \mathbf{c}^{(k)}. \quad (5)$$

The right-hand-side can be concretized by Eq. (2) to serve as an approximation for $V(\cdot)$ after the branching. In this way, the linear bounds are directly propagated from node i to input \mathbf{x} and concretized using a shortcut. We thereby take the concretized bound as $\tilde{V}(\mathbf{l}, \mathbf{u}, i, j, k, \mathbf{p}_{i,j})$ for our BBPS heuristic score.

Our branching heuristic is generally formulated. We leverage updates on the linear relaxation of any nonlinearity, and general branching points and general number of inputs nodes are supported when we update the linear relaxation. Node i can also have multiple output nodes which are nonlinearities, where we accumulate the linear bounds propagated from all the output nodes in Eq. (3).

Comparison to previous works. Existing branching heuristics from previous works (Bunel et al., 2018, 2020; Lu & Mudigonda, 2020; De Palma et al., 2021) are more restrictive, as they mostly focused on branching ReLU neurons with a fixed branching point (0 for ReLU) and their heuristic is specifically formulated for ReLU, unlike our general formulation above. We also empirically find they are often not precise enough on general nonlinearities due to their

approximations. In the existing BaBSR heuristic originally for ReLU networks (Bunel et al., 2020), they essentially propagate the bounds only to the node before the branched one with an early stop, and they then ignore the coefficients ($\mathbf{A}_{i-1,j}^{(k)}$ for a feedforward NN) without propagating further. In contrast, in our BBPS heuristic, we carefully utilize a shortcut to propagate the bounds to the input as Eq. (5) rather than discard linear terms early. Therefore, we expect our BBPS heuristic to be more precise and effective, while it does not increase the complexity with the efficient shortcut.

3.4 Where to Branch? New Considerations for General Nonlinear Functions

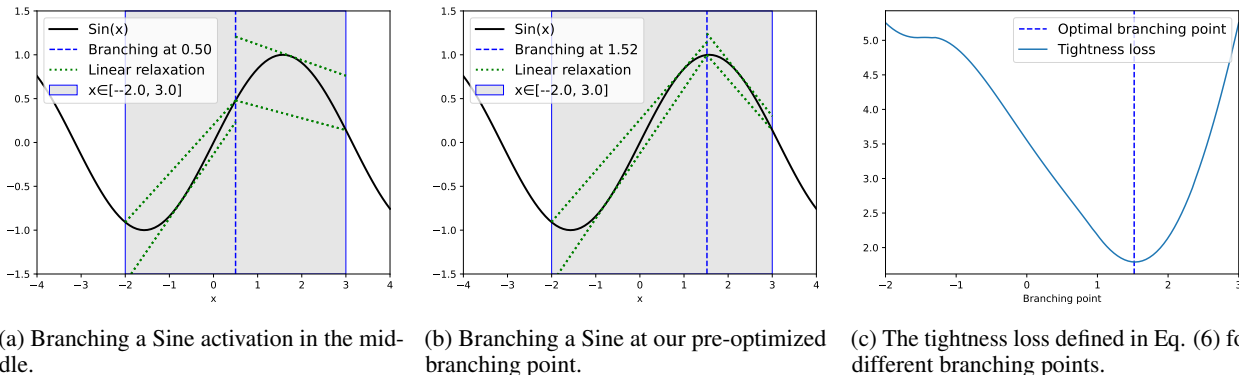


Figure 2: Illustration of branching the intermediate bounds of a neuron connected to the Sine activation (Sitzmann et al., 2020).

The more complex nature of general nonlinear functions also brings flexibility on choosing branching points, compared to the ReLU activation where only branching at 0 is reasonable. A straightforward way is to branch in the middle between the intermediate lower and upper bounds, as shown in Figure 2a. However, this can be suboptimal for many nonlinear functions. In contrast, we perform an optimization offline for each case of nonlinearities before running our BaB. We also consider cases where multiple nonlinearities are connected to same node as shown in Figure 1. We enumerate all pairs of possible intermediate bounds within a certain range with a step size, where we set a small step size which defines the gap between the adjacent enumerated intermediate bounds. We save the optimized branching points into a lookup table. During verification, for each pair of intermediate bounds we actually encounter, we efficiently query the lookup table and take the branching point for the closest intermediate bound pair in the lookup table (if no valid branching point is obtained from the lookup table, we try branching in the middle instead, as a backup). We call it “pre-optimized branching points”, as an example shown in Figure 2b.

For simplicity here, we mainly assume that we have a unary nonlinear function $q(x)$, although our method supports functions with any number of inputs in practice. Suppose the input intermediate bounds for $q(x)$ is $l \leq x \leq u$, we aim to find a branching point $p = P(l, u)$ such that the overall tightness of the linear relaxation for input range $[l, p]$ and $[p, u]$, respectively, is the best. Suppose the linear relaxation for input range $[l, p]$ is $\underline{a}_1x + \underline{b}_1 \leq q(x) \leq \bar{a}_1x + \bar{b}_1$, and similarly $\underline{a}_2x + \underline{b}_2 \leq q(x) \leq \bar{a}_2x + \bar{b}_2$ for input range $[p, u]$. Following previous works such as Shi et al. (2020), we use the integral of the gap between the lower linear relaxation and the upper linear relaxation to measure the tightness (the linear relaxation is considered as tighter when the gap is smaller). We define it as a *tightness loss* $P(q(x), l, u, p)$ for nonlinearity $q(x)$ with input range $[l, u]$ and branching point p :

$$P(q(x), l, u, p) = \int_l^p \left((\bar{a}_1x + \bar{b}_1) - (\underline{a}_1x + \underline{b}_1) \right) dx + \int_p^u \left((\bar{a}_2x + \bar{b}_2) - (\underline{a}_2x + \underline{b}_2) \right) dx, \quad (6)$$

where the parameters for the linear relaxation ($\underline{a}_1, \bar{a}_1, \underline{b}_1, \bar{b}_1, \underline{a}_2, \bar{a}_2, \underline{b}_2, \bar{b}_2$) all depend on p . We take the best branching point p ($l < p < u$) which minimizes $P(q(x), l, u, p)$. Figure 2c plots the tightness loss for the Sine activation. This problem can be solved by gradient descent, or an enumeration over a number of potential branching points if the nonlinear function only has one or two inputs.

Moreover, we also support a generalized version of Eq. (6) for nonlinear functions with multiple inputs (such as multiplication involving two inputs), where we use a multiple integral to measure the tightness for multi-dimensional nonlinearities. And when a branched node has multiple nonlinear output nodes, we take the sum for multiple nonlinearities as $\sum_{q \in \mathcal{Q}} P(q(x), l, u, p)$, where \mathcal{Q} is the set of output nonlinearities. As such, our pre-optimized branching points support general computational graphs.

4 Experiments

Table 1: List of models with various nonlinearities in our experiments.

Model	Nonlinearities in the model
Feedforward	sigmoid, tanh, sin, GeLU
LSTM	sigmoid, tanh, xy
ViT with ReLU	ReLU, xy , x/y , x^2 , \sqrt{x} , $\exp(x)$
ML4ACOPF	ReLU, sigmoid, sin, xy , x^2

Models and Data. We focus on verifying NNs with nonlinearities beyond ReLU, and we experiment on models with various nonlinearities as shown in Table 1. We mainly consider the commonly used ℓ_∞ robustness verification specification on image classification. We adopt some MNIST (LeCun et al., 2010) models with Sigmoid and Tanh activation functions from previous works (Singh et al., 2019a,b; Müller et al., 2022), along with their data instances. Besides, we train many new models with various nonlinearities on CIFAR-10 (Krizhevsky et al., 2009) by PGD adversarial training (Madry et al., 2018), using an ℓ_∞ perturbation with $\epsilon = 1/255$ in both training and verification. For these CIFAR-10 models, we first run vanilla CROWN (Zhang et al., 2020; Xu et al., 2020), i.e., CROWN without optimized linear relaxation (Xu et al., 2021; Lyu et al., 2020) or BaB (Xu et al., 2021; Wang et al., 2021), to remove instances which are too easy where vanilla CROWN already succeeds. We also remove instances where PGD attack succeeds, as such instances are impossible to verify. We only retain the first 100 instances if there are more instances left. We set a timeout of 300 seconds for our BaB in all these experiments. In addition, we adopt an NN verification benchmark for verifying properties in the Machine Learning for AC Optimal Power Flow (ML4ACOPF) problem (Guha et al., 2019)² which is beyond robustness verification. For completeness, we also show results on a ReLU network in Appendix B.2. Additional details are in Appendix C.

Baselines. We compare our GenBaB with the previous α, β -CROWN which does not support BaB on non-ReLU nonlinearities. We also compare with several other baselines, including DeepPoly (Singh et al., 2019b), PRIMA (Müller et al., 2022), VeriNet (Henriksen & Lomuscio, 2020), PROVER (Ryou et al., 2021), DeepT (Bonaert et al., 2021), Wu et al. (2022), Wei et al. (2023), on the models they support, respectively. Among these baselines, only VeriNet and Wu et al. (2022) support BaB on Sigmoid or Tanh models, and none of the baseline supports BaB on general nonlinearities. While the original BaBSR heuristic in Bunel et al. (2020) only supported ReLU networks, we also implemented a generalized version of BaBSR for nonlinearities beyond ReLU for an empirical comparison in Table 3, based on the difference in treating the linear term discussed in Section 3.3.

Experiments on Sigmoid and Tanh networks for MNIST. We first experiment on Sigmoid networks and Tanh networks for MNIST and show the results in Table 2. On 6 out of the 8 models, our GenBaB is able to verify more instances over α, β -CROWN without BaB and also outperforms all the non-CROWN baselines. We find that improving on Sigmoid 9×100 and Tanh 6×100 networks by BaB is harder, as the initial bounds are typically too loose on the unverifiable instances before BaB, possibly due to these models being trained without robustness consideration.

Experiments on feedforward networks with various activation functions on CIFAR-10. In Table 3 and Figure 3, we show results for models on CIFAR-10. On all the models, GenBaB verifies much more instances compared to α, β -CROWN without BaB. We also conduct ablation studies to investigate the effect of our BBPS heuristic and branching points, with results shown in the last three rows of Table 3. Comparing “Base BaB” and “+ BBPS”, on most of the models, we find that our BBPS heuristic significantly improves over directly generalizing the BaBSR heuristic (Bunel et al., 2020) used in “Base BaB”. Comparing “+ BBPS” and “+ BBPS, + pre-optimized”, we find that our pre-optimized branching points achieve a noticeable improvement on many models over always branching in the middle used in “+ BBPS”. The results demonstrate the effectiveness of our GenBaB with our BBPS heuristic and pre-optimized branching points. For PRIMA and vanilla CROWN, as we only use relatively hard instances for verification here, these two methods are unable to verify any instance in this experiment. For VeriNet, all the models here are too large without a license for the FICO Xpress solver (we are unable to obtain an academic license as mentioned in Table 2); we have not obtained the code to run Wu et al. (2022) on these models either. Thus, we do not include the results for VeriNet or Wu et al. (2022).

Experiments on LSTMs. Next, we experiment on LSTMs containing more complex nonlinearities, including both Sigmoid and Tanh activations, as well as multiplication as $\text{sigmoid}(x) \tanh(y)$ and $\text{sigmoid}(x)y$. We compare with PROVER (Ryou et al., 2021) which is a specialized for RNNs and it outperforms earlier works (Ko et al., 2019). While

²Repository for the ML4ACOPF benchmark: https://github.com/AI4OPT/ml4acopf_benchmark.

Table 2: Number of verified instances out of the first 100 test examples on MNIST for several Sigmoid networks and Tanh networks along with their ϵ . The settings are the same as those in PRIMA (Müller et al., 2022). “ $L \times W$ ” in the network names denote a fully-connected NN with L layers and W hidden neurons in each layer. The upper bounds in the last row are computed by PGD attack (Madry et al., 2018), as a sound verification should not verify instances where PGD can successfully find counterexamples.

Method	Sigmoid Networks				Tanh Networks			
	6×100 $\epsilon=0.015$	6×200 $\epsilon=0.012$	9×100 $\epsilon=0.015$	ConvSmall $\epsilon=0.014$	6×100 $\epsilon=0.006$	6×200 $\epsilon=0.002$	9×100 $\epsilon=0.006$	ConvSmall $\epsilon=0.005$
DeepPoly ^{ab}	30	43	38	30	38	39	18	16
PRIMA ^a	53	73	56	51	61	68	52	30
VeriNet ^c	65	81	56	-	31	30	16	-
Wu et al. (2022) [?]	65	75	96 [?]	63	-	-	-	-
Vanilla CROWN ^b	53	63	49	65	18	24	44	55
α, β -CROWN (w/o BaB)	62	81	62	84	65	72	58	69
GenBaB (ours)	71	83	62	92	65	78	59	75
Upper bound	93	99	92	97	94	97	96	98

^aResults for DeepPoly and PRIMA are directly from Müller et al. (2022).

^bWhile DeepPoly and CROWN are thought to be equivalent on ReLU networks (Müller et al., 2022), these two works adopt different relaxation for Sigmoid and Tanh, which results in different results here.

^cResults for VeriNet are obtained by running the tool (<https://github.com/vas-group-imperial/VeriNet>) by ourselves. VeriNet depends on the FICO Xpress commercial solver which requires a license for models that are relatively large. FICO Xpress declined the request we submitted for the academic license, directing us to obtain it via a (course) tutor, which is not applicable to our research. Thus results on ConvSmall models are not available.

[?]We found that the result Wu et al. (2022) reported on the Sigmoid 9×100 model exceeds the upper bound by PGD attack ($96 > 92$), and thus the result tends to be not fully valid. Results on Tanh networks are unavailable.

Table 3: Number of verified instances out of 100 filtered instances on CIFAR-10 with $\epsilon = 1/255$ for feedforward networks with various activation functions. The last three rows contain results for the ablation study, where “Base BaB” does not use our BBPS heuristic or pre-optimized branching points, but it uses a generalized BaBSR heuristic (Bunel et al., 2020) and always branches intermediate bounds $[l, u]$ in the middle into $[l, \frac{l+u}{2}]$ and $[\frac{l+u}{2}, u]$.

Method	Sigmoid Networks				Tanh Networks		Sine Networks			GeLU Networks		
	4×100	4×500	6×100	6×200	4×100	6×100	4×100	4×200	4×500	4×100	4×200	4×500
PRIMA ^a	0	0	0	0	0	0	-	-	-	-	-	-
Vanilla CROWN ^b	0	0	0	0	0	0	0	0	0	0	0	0
α, β -CROWN (w/o BaB) ^c	28	16	43	39	25	6	4	2	4	44	33	27
GenBaB (ours)	58	24	64	50	49	10	60	35	22	82	65	39
Ablation Studies												
Base BaB	34	19	44	41	34	8	9	8	7	64	54	39
+ BBPS	57	24	63	49	48	10	56	34	21	74	59	36
+ BBPS, + pre-optimized	58	24	64	50	49	10	60	35	22	82	65	39

^aResults for PRIMA are obtained by running ERAN (<https://github.com/eth-sri/eran>) which contains PRIMA. PRIMA does not support Sine or GeLU activations.

^bWe have extended the support of vanilla CROWN to GeLU, as discussed in Appendix A.3.

^cWe have extended optimizable linear relaxation in α, β -CROWN to Sine and GeLU, as discussed in Appendix A.

there are other works on verifying RNN and LSTM, such as Du et al. (2021); Mohammadnejad et al. (2021); Paulsen & Wang (2022), we have not obtained their code, and we also make orthogonal contributions compared to them on improving the relaxation for RNN verification which can also be combined with our BaB. We take the hardest model, an LSTM for MNIST, from the main experiments of PROVER (other models can be verified by PROVER on more than 90% instances and are thus omitted), where each 28×28 image is sliced into 7 frames for LSTM. We also have two LSTMs trained by ourselves on CIFAR-10, where we linearly map each 32×32 image into 4 patches as the input tokens, similar to ViTs with patches (Dosovitskiy et al., 2021). Table 4 shows the results. α, β -CROWN without BaB can already outperform PROVER with specialized relaxation for RNN and LSTM. Our GenBaB outperforms both PROVER and α, β -CROWN without BaB.

Experiments on ViTs. We also experiment on ViTs which contain more other nonlinearities, as shown in Table 1. For ViTs, we compare with DeepT (Bonaert et al., 2021) which is specialized for verifying Transformers without BaB. We show the results in Table 4, where our methods outperform DeepT, and BaB effectively improves the verification. Using our pre-optimized branching points also brings a noticeable improvement compared to branching in the middle.

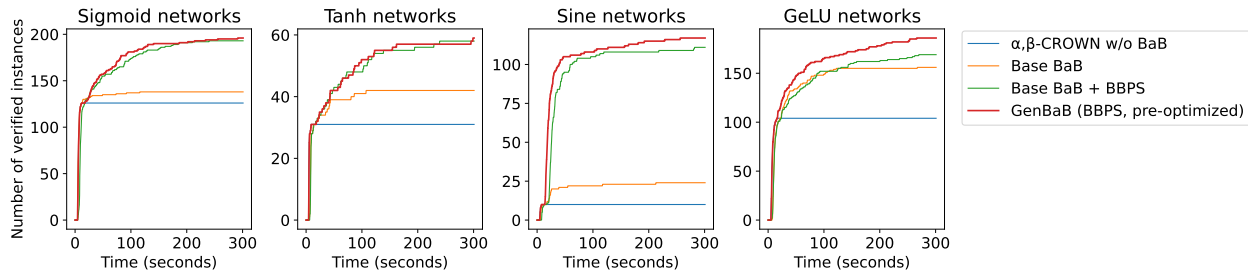


Figure 3: Total number of verified instances against running time threshold on feedforward networks for CIFAR-10 with various activation functions. “Base BaB” means that in the most basic BaB setting, where we use a generalized BaBSR heuristic and always branch in the middle point of intermediate bounds. “Base + BBPS” uses our BBPS heuristic. Our full GenBaB uses both BBPS and pre-optimized branching points.

Table 4: Number of verified instances out of 100 instances on LSTMs and ViTs. The MNIST model is from PROVER (Ryou et al., 2021) with $\epsilon = 0.01$, and the CIFAR-10 models are trained by ourselves with $\epsilon = 1/255$. “LSTM-7-32” indicates an LSTM with 7 input frames and 32 hidden neurons, similar for the other two models. “ViT- L - H ” stands for L layers and H heads. Some models have fewer than 100 instances, after filtering out easy or impossible instances, as shown in “upper bounds”. Results for PROVER are obtained by running the tool (<https://github.com/eth-sri/prover>). Results for DeepT are obtained by running the tool (<https://github.com/eth-sri/DeepT>). PROVER and DeepT specialize in RNNs and ViTs, respectively. We also show results when we branch in the middle without using our pre-optimized branching points (“GenBaB w/o pre-optimized”).

Method	MNIST Model		CIFAR-10 Models				
	LSTM-7-32	LSTM-4-32	LSTM-4-64	ViT-1-3	ViT-1-6	ViT-2-3	ViT-2-6
PROVER	63	8	3	-	-	-	-
DeepT	-	-	-	0	1	0	1
α, β -CROWN w/o BaB	82	16	9	1	3	11	7
GenBaB w/o pre-optimized	84	19	13	29	33	36	25
GenBaB	84	20	14	39	44	37	27
Upper bound	98	100	100	67	92	72	69

Moreover, in Appendix B.1, we compare with Wei et al. (2023) which supports verifying attention networks but not the entire ViT, and we experiment on models from Wei et al. (2023), where our methods also outperform Wei et al. (2023).

Experiments on ML4ACOPF. Finally, we experiment on models for the Machine Learning for AC Optimal Power Flow (ML4ACOPF) problem (Guha et al., 2019), and we adopt the ML4ACOPF neural network verification benchmark, a standardized benchmark in the 2023 International Verification of Neural Networks Competition (VNN-COMP’23). The benchmark consists of a NN with power demands as inputs, and the output of the NN gives an operation plan of electric power plants. Then, the benchmark aims to check for a few nonlinear constraint violations of this plan, such as power generation and balance constraints. These constraints, as part of the computational graph to verify, involve many nonlinearities including Sine, Sigmoid, multiplication, and square function. Our framework is the first to support this verification problem. Among the 23 benchmark instances, PGD attack only succeeds on one instance, and our BaB verifies all the remaining 22 instances; without BaB, optimizing α only can verify only 16 instances in this benchmark. This shows a more practical application of our work and further demonstrates the effectiveness of our framework.

5 Related Work

Branch-and-bound (BaB) has been shown to be an effective technique for NN verification (Bunel et al., 2018; Lu & Mudigonda, 2020; Wang et al., 2018a; Xu et al., 2021; De Palma et al., 2021; Kouvaros & Lomuscio, 2021; Wang et al., 2021; Henriksen & Lomuscio, 2021; Shi et al., 2022), but most of the existing works focus on ReLU networks and are not directly applicable to networks with nonlinearities beyond ReLU. On BaB for NNs with other nonlinearities, Henriksen & Lomuscio (2020) conducted BaB on Sigmoid and Tanh networks, but their framework depends on a commercial LP solver which has been argued as less effective than recent NN verification methods using linear bound propagation with branching constraints (Wang et al., 2021). Besides, Wu et al. (2022) studied verifying Sigmoid networks with counter-example-guided abstraction refinement. These works have only considered S-shaped activations, and there lacks

a general framework supporting general nonlinearities beyond a particular type of activation functions, which we address in this paper. Without using BaB, there are many works studying the verification for NNs with various nonlinearities, by improving the relaxation or extending the support of verification to various architectures: Sigmoid networks (Choi et al., 2023), RNNs and LSTMs (Ko et al., 2019; Du et al., 2021; Ryou et al., 2021; Mohammadinejad et al., 2021; Zhang et al., 2023; Tran et al., 2023), and Transformers (Shi et al., 2019; Bonaert et al., 2021; Wei et al., 2023; Zhang et al., 2024). These works have orthogonal contributions compared to ours using BaB for further improvement above a base verifier. In addition, there are works studying the branching heuristic in verifying ReLU networks, such as filtering initial candidates with a more accurate computation (De Palma et al., 2021), using Graph Neural Networks for the heuristic (Lu & Mudigonda, 2020), or using a heuristic guided with tighter multiple-neuron relaxation (Ferrari et al., 2021), which may inspire future improvement on the BaB for general nonlinearities.

6 Conclusions

To conclude, we propose a general BaB framework for NN verification involving general nonlinearities in general computational graphs. We also propose a new branching heuristic for deciding branched neurons and an offline optimization procedure for deciding branching points. Experiments on verifying NNs with various nonlinearities demonstrate the effectiveness of our method. We believe our work can enable more applications of NN verification involving various nonlinearities.

Limitations and future work. Although we have demonstrated a practical application on ML4ACOPF, most of our experiments have focused on the typical robustness verification for image classifiers. We believe our work has the potential for broader applications requiring formally verifying neural networks in various other domains, which will be interesting for future works. In addition, many models we have demonstrated are still much smaller than those deployed in large-scale machine learning applications, which is also a common limitation of current NN verification methods. Further scaling up NN verification to larger models will be important for future works.

Acknowledgments

This project is supported in part by NSF 2048280, 2331966, 2331967 and ONR N00014-23-1-2300:P00001. Huan Zhang is supported in part by the AI2050 program at Schmidt Sciences (Grant #G-23-65921).

References

- Bonaert, G., Dimitrov, D. I., Baader, M., and Vechev, M. Fast and precise certification of transformers. In *Proceedings of the 42nd ACM SIGPLAN International Conference on Programming Language Design and Implementation*, pp. 466–481, 2021.
- Brix, C., Bak, S., Liu, C., and Johnson, T. T. The fourth international verification of neural networks competition (vnn-comp 2023): Summary and results. *arXiv preprint arXiv:2312.16760*, 2023.
- Bunel, R., Turkaslan, I., Torr, P. H. S., Kohli, P., and Mudigonda, P. K. A unified view of piecewise linear neural network verification. In *Advances in Neural Information Processing Systems*, pp. 4795–4804, 2018.
- Bunel, R., Mudigonda, P., Turkaslan, I., Torr, P., Lu, J., and Kohli, P. Branch and bound for piecewise linear neural network verification. *Journal of Machine Learning Research*, 21(2020), 2020.
- Choi, S. W., Ivashchenko, M., Nguyen, L. V., and Tran, H.-D. Reachability analysis of sigmoidal neural networks. *ACM Transactions on Embedded Computing Systems*, 2023.
- De Palma, A., Bunel, R., Desmaison, A., Dvijotham, K., Kohli, P., Torr, P. H., and Kumar, M. P. Improved branch and bound for neural network verification via lagrangian decomposition. *arXiv preprint arXiv:2104.06718*, 2021.
- Dosovitskiy, A., Beyer, L., Kolesnikov, A., Weissenborn, D., Zhai, X., Unterthiner, T., Dehghani, M., Minderer, M., Heigold, G., Gelly, S., Uszkoreit, J., and Houlsby, N. An image is worth 16x16 words: Transformers for image recognition at scale. In *International Conference on Learning Representations*, 2021.
- Du, T., Ji, S., Shen, L., Zhang, Y., Li, J., Shi, J., Fang, C., Yin, J., Beyah, R., and Wang, T. Cert-rnn: Towards certifying the robustness of recurrent neural networks. In *Proceedings of the 2021 ACM SIGSAC Conference on Computer and Communications Security, CCS '21*, pp. 516–534, 2021. ISBN 9781450384544. doi: 10.1145/3460120.3484538.

- Dvijotham, K., Stanforth, R., Gowal, S., Mann, T. A., and Kohli, P. A dual approach to scalable verification of deep networks. In *Proceedings of the Thirty-Fourth Conference on Uncertainty in Artificial Intelligence, UAI 2018, Monterey, California, USA, August 6-10, 2018*, pp. 550–559, 2018.
- Ferrari, C., Mueller, M. N., Jovanović, N., and Vechev, M. Complete verification via multi-neuron relaxation guided branch-and-bound. In *International Conference on Learning Representations*, 2021.
- Guha, N., Wang, Z., Wytoczek, M., and Majumdar, A. Machine learning for ac optimal power flow. *arXiv preprint arXiv:1910.08842*, 2019.
- Henriksen, P. and Lomuscio, A. Efficient neural network verification via adaptive refinement and adversarial search. In *ECAI 2020*, pp. 2513–2520. IOS Press, 2020.
- Henriksen, P. and Lomuscio, A. Deepsplit: An efficient splitting method for neural network verification via indirect effect analysis. In *IJCAI*, pp. 2549–2555, 2021.
- Hochreiter, S. and Schmidhuber, J. Long short-term memory. *Neural computation*, 9(8):1735–1780, 1997.
- Katz, G., Barrett, C., Dill, D. L., Julian, K., and Kochenderfer, M. J. Reluplex: An efficient smt solver for verifying deep neural networks. In *International Conference on Computer Aided Verification*, pp. 97–117, 2017.
- Ko, C., Lyu, Z., Weng, L., Daniel, L., Wong, N., and Lin, D. POPQORN: quantifying robustness of recurrent neural networks. In *International Conference on Machine Learning*, volume 97 of *Proceedings of Machine Learning Research*, pp. 3468–3477, 2019.
- Kouvaros, P. and Lomuscio, A. Towards scalable complete verification of relu neural networks via dependency-based branching. In *IJCAI*, pp. 2643–2650, 2021.
- Krizhevsky, A., Hinton, G., et al. Learning multiple layers of features from tiny images. *Technical Report TR-2009*, 2009.
- LeCun, Y., Cortes, C., and Burges, C. Mnist handwritten digit database. *ATT Labs [Online]*. Available: <http://yann.lecun.com/exdb/mnist>, 2, 2010.
- Lu, J. and Mudigonda, P. Neural network branching for neural network verification. In *Proceedings of the International Conference on Learning Representations (ICLR 2020)*. Open Review, 2020.
- Lyu, Z., Ko, C., Kong, Z., Wong, N., Lin, D., and Daniel, L. Fastened CROWN: tightened neural network robustness certificates. In *The Thirty-Fourth AAAI Conference on Artificial Intelligence*, pp. 5037–5044, 2020.
- Madry, A., Makelov, A., Schmidt, L., Tsipras, D., and Vladu, A. Towards deep learning models resistant to adversarial attacks. In *International Conference on Learning Representations*, 2018.
- Mohammadinejad, S., Paulsen, B., Deshmukh, J. V., and Wang, C. Diffrrn: Differential verification of recurrent neural networks. In *Formal Modeling and Analysis of Timed Systems: 19th International Conference, FORMATS 2021, Paris, France, August 24–26, 2021, Proceedings 19*, pp. 117–134. Springer, 2021.
- Müller, M. N., Makarchuk, G., Singh, G., Püschel, M., and Vechev, M. Prima: general and precise neural network certification via scalable convex hull approximations. *Proceedings of the ACM on Programming Languages*, 6(POPL): 1–33, 2022.
- Paulsen, B. and Wang, C. Linsyn: Synthesizing tight linear bounds for arbitrary neural network activation functions. In *Tools and Algorithms for the Construction and Analysis of Systems: 28th International Conference, TACAS 2022, Held as Part of the European Joint Conferences on Theory and Practice of Software, ETAPS 2022, Munich, Germany, April 2–7, 2022, Proceedings, Part I*, pp. 357–376. Springer, 2022.
- Ryou, W., Chen, J., Balunovic, M., Singh, G., Dan, A., and Vechev, M. Scalable polyhedral verification of recurrent neural networks. In *International Conference on Computer Aided Verification*, pp. 225–248, 2021.
- Shi, Z., Zhang, H., Chang, K.-W., Huang, M., and Hsieh, C.-J. Robustness verification for transformers. In *International Conference on Learning Representations*, 2019.
- Shi, Z., Zhang, H., Chang, K., Huang, M., and Hsieh, C. Robustness verification for transformers. In *International Conference on Learning Representations*, 2020.

- Shi, Z., Wang, Y., Zhang, H., Kolter, J. Z., and Hsieh, C.-J. Efficiently computing local lipschitz constants of neural networks via bound propagation. *Advances in Neural Information Processing Systems*, 35:2350–2364, 2022.
- Singh, G., Ganvir, R., Püschel, M., and Vechev, M. T. Beyond the single neuron convex barrier for neural network certification. In *Advances in Neural Information Processing Systems*, pp. 15072–15083, 2019a.
- Singh, G., Gehr, T., Püschel, M., and Vechev, M. An abstract domain for certifying neural networks. *Proceedings of the ACM on Programming Languages*, 3(POPL):41, 2019b.
- Sitzmann, V., Martel, J., Bergman, A., Lindell, D., and Wetzstein, G. Implicit neural representations with periodic activation functions. *Advances in Neural Information Processing Systems*, 33:7462–7473, 2020.
- Tran, H. D., Choi, S. W., Yang, X., Yamaguchi, T., Hoxha, B., and Prokhorov, D. Verification of recurrent neural networks with star reachability. In *Proceedings of the 26th ACM International Conference on Hybrid Systems: Computation and Control*, pp. 1–13, 2023.
- Vaswani, A., Shazeer, N., Parmar, N., Uszkoreit, J., Jones, L., Gomez, A. N., Kaiser, L., and Polosukhin, I. Attention is all you need. In *Advances in Neural Information Processing Systems 30: Annual Conference on Neural Information Processing Systems 2017, December 4-9, 2017, Long Beach, CA, USA*, pp. 5998–6008, 2017.
- Wang, S., Pei, K., Whitehouse, J., Yang, J., and Jana, S. Efficient formal safety analysis of neural networks. In *Advances in Neural Information Processing Systems*, pp. 6369–6379, 2018a.
- Wang, S., Pei, K., Whitehouse, J., Yang, J., and Jana, S. Formal security analysis of neural networks using symbolic intervals. In *27th {USENIX} Security Symposium ({USENIX} Security 18)*, pp. 1599–1614, 2018b.
- Wang, S., Zhang, H., Xu, K., Lin, X., Jana, S., Hsieh, C.-J., and Kolter, J. Z. Beta-crown: Efficient bound propagation with per-neuron split constraints for neural network robustness verification. *Advances in Neural Information Processing Systems*, 34:29909–29921, 2021.
- Wei, D., Wu, H., Wu, M., Chen, P.-Y., Barrett, C., and Farchi, E. Convex bounds on the softmax function with applications to robustness verification. In *International Conference on Artificial Intelligence and Statistics*, pp. 6853–6878. PMLR, 2023.
- Wong, E. and Kolter, J. Z. Provable defenses against adversarial examples via the convex outer adversarial polytope. In *International Conference on Machine Learning*, volume 80 of *Proceedings of Machine Learning Research*, pp. 5283–5292, 2018.
- Wu, H., Tagomori, T., Robey, A., Yang, F., Matni, N., Pappas, G., Hassani, H., Pasareanu, C., and Barrett, C. Toward certified robustness against real-world distribution shifts. *arXiv preprint arXiv:2206.03669*, 2022.
- Xu, K., Shi, Z., Zhang, H., Wang, Y., Chang, K., Huang, M., Kailkhura, B., Lin, X., and Hsieh, C. Automatic perturbation analysis for scalable certified robustness and beyond. In *Advances in Neural Information Processing Systems*, 2020.
- Xu, K., Zhang, H., Wang, S., Wang, Y., Jana, S., Lin, X., and Hsieh, C. Fast and complete: Enabling complete neural network verification with rapid and massively parallel incomplete verifiers. In *International Conference on Learning Representations*, 2021.
- Zhang, H., Weng, T., Chen, P., Hsieh, C., and Daniel, L. Efficient neural network robustness certification with general activation functions. In *Advances in Neural Information Processing Systems*, pp. 4944–4953, 2018.
- Zhang, H., Chen, H., Xiao, C., Gowal, S., Stanforth, R., Li, B., Boning, D. S., and Hsieh, C. Towards stable and efficient training of verifiably robust neural networks. In *International Conference on Learning Representations*, 2020.
- Zhang, Y., Du, T., Ji, S., Tang, P., and Guo, S. Rnn-guard: Certified robustness against multi-frame attacks for recurrent neural networks. *arXiv preprint arXiv:2304.07980*, 2023.
- Zhang, Y., Shen, L., Guo, S., and Ji, S. Galileo: General linear relaxation framework for tightening robustness certification of transformers. In *Proceedings of the AAAI Conference on Artificial Intelligence*, volume 38, pp. 21797–21805, 2024.

A Additional Optimizable Linear Relaxation

In this section, we derive new optimizable linear relaxation for nonlinearities including multiplication, sine, and GeLU, which are not originally supported in α, β -CROWN for optimizable linear relaxation.

A.1 Optimizable Linear Relaxation for Multiplication

For each elementary multiplication xy where $x \in [\underline{x}, \bar{x}]$, $y \in [\underline{y}, \bar{y}]$ are the intermediate bounds for x and y , we aim to relax and bound xy as:

$$\forall x \in [\underline{x}, \bar{x}], y \in [\underline{y}, \bar{y}], \quad \underline{a}x + \underline{b}y + \underline{c} \leq xy \leq \bar{a}x + \bar{b}y + \bar{c}, \quad (7)$$

where $\underline{a}, \underline{b}, \underline{c}, \bar{a}, \bar{b}, \bar{c}$ are parameters in the linear bounds. Shi et al. (2019) derived optimal parameters that minimize the gap between the relaxed upper bound and the relaxed lower bound:

$$\begin{aligned} \arg \min_{\underline{a}, \underline{b}, \underline{c}, \bar{a}, \bar{b}, \bar{c}} \int_{x \in [\underline{x}, \bar{x}]} \int_{y \in [\underline{y}, \bar{y}]} (\bar{a}x + \bar{b}y + \bar{c}) - (\underline{a}x + \underline{b}y + \underline{c}) \\ \text{s.t. Eq. (7) holds.} \end{aligned} \quad (8)$$

However, the optimal parameters they found only guarantee that the linear relaxation is optimal for this node, but not the final bounds after conducting a bound propagation on the entire NN. Therefore, we aim to make these parameters optimizable to tighten the final bounds as previous works did for ReLU networks or S-shaped activations (Xu et al., 2021; Lyu et al., 2020).

We notice that Shi et al. (2019) mentioned that there are two solutions for $\underline{a}, \underline{b}, \underline{c}$ and $\bar{a}, \bar{b}, \bar{c}$ respectively that solves Eq. (8):

$$\begin{cases} \underline{a}_1 = \underline{y} \\ \underline{b}_1 = \underline{x} \\ \underline{c}_1 = -\underline{x}\underline{y} \end{cases}, \quad \begin{cases} \bar{a}_1 = \bar{y} \\ \bar{b}_1 = \underline{x} \\ \bar{c}_1 = -\underline{x}\bar{y} \end{cases}, \quad (9)$$

$$\begin{cases} \underline{a}_2 = \bar{y} \\ \underline{b}_2 = \bar{x} \\ \underline{c}_2 = -\bar{x}\underline{y} \end{cases}, \quad \begin{cases} \bar{a}_2 = \underline{y} \\ \bar{b}_2 = \bar{x} \\ \bar{c}_2 = -\bar{x}\bar{y} \end{cases}. \quad (10)$$

Therefore, to make the parameters optimizable, we introduce parameters $\underline{\alpha}$ and $\bar{\alpha}$, and we interpolate between Eq. (9) and Eq. (10) as:

$$\begin{cases} \underline{a} = \underline{\alpha}\underline{y} + (1 - \underline{\alpha})\bar{y} \\ \underline{b} = \underline{\alpha}\underline{x} + (1 - \underline{\alpha})\bar{x} \\ \underline{c} = -\underline{\alpha}\underline{x}\underline{y} - (1 - \underline{\alpha})\bar{x}\bar{y} \end{cases} \quad \text{s.t. } 0 \leq \underline{\alpha} \leq 1, \quad (11)$$

$$\begin{cases} \bar{a} = \bar{\alpha}\bar{y} + (1 - \bar{\alpha})\underline{y} \\ \bar{b} = \bar{\alpha}\bar{x} + (1 - \bar{\alpha})\underline{x} \\ \bar{c} = -\bar{\alpha}\bar{x}\bar{y} - (1 - \bar{\alpha})\underline{x}\underline{y} \end{cases} \quad \text{s.t. } 0 \leq \bar{\alpha} \leq 1. \quad (12)$$

It is easy to verify that interpolating between two sound linear relaxations satisfying Eq. (7) still yields a sound linear relaxation. And $\underline{\alpha}$ and $\bar{\alpha}$ are part of all the optimizable linear relaxation parameters α mentioned in Section 2.

A.2 Optimizable Linear Relaxation for Sine

We also derive new optimized linear relaxation for periodic functions, in particular $\sin(x)$. For $\sin(x)$ where $x \in [\underline{x}, \bar{x}]$, we aim to relax and bound $\sin(x)$ as:

$$\forall x \in [\underline{x}, \bar{x}], \quad \underline{a}x + \underline{b} \leq \sin(x) \leq \bar{a}x + \bar{b}, \quad (13)$$

where $\underline{a}, \underline{b}, \bar{a}, \bar{b}$ are parameters in the linear bounds. A non-optimizable linear relaxation for \sin already exists in α, β -CROWN and we adopt it as an initialization and focus on making it optimizable. At initialization, we first check the line connecting $(\underline{x}, \sin(\underline{x}))$ and $(\bar{x}, \sin(\bar{x}))$, and this line is adopted as the lower bound or the upper bound without further optimization, if it is a sound bounding line.

Otherwise, a tangent line is used as the bounding line with the tangent point being optimized. Within $[\underline{x}, \bar{x}]$, if $\sin(x)$ happens to be monotonic with at most only one inflection point, the tangent point can be optimized in a way similar to bounding an S-shaped activation (Lyu et al., 2020), as illustrated in Figure 4.

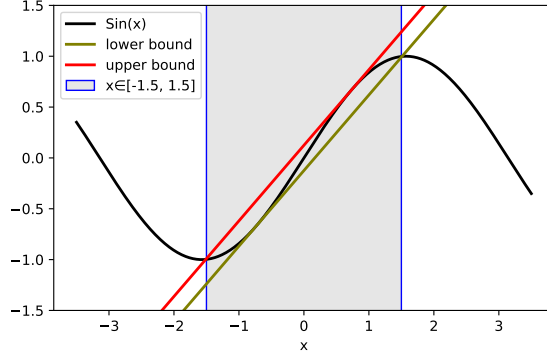


Figure 4: Linear relaxation for a Sin activation in an input range $[-1.5, 1.5]$ where the function is S-shaped.

Otherwise, there are multiple extreme points within the input range. Initially, we aim to find a tangent line that passes $(\underline{x}, \sin(\underline{x}))$ as the bounding line. Since \underline{x} may be at different cycles of the sin function, we project into the cycle with range $[-0.5\pi, 1.5\pi]$, by taking $\tilde{\underline{x}}_l = \underline{x} - 2k_l\pi$, where $k_l = \lfloor \frac{\underline{x} + 0.5\pi}{2\pi} \rfloor$. With a binary search, we find a tangent point $\underline{\alpha}_l$ on the projected cycle that satisfies

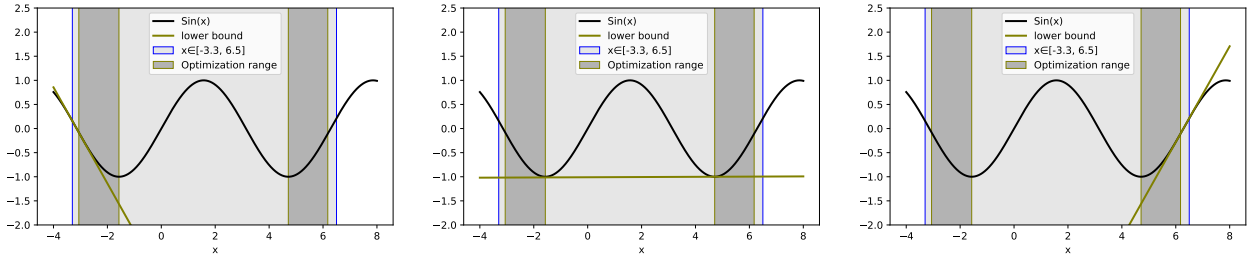
$$\sin'(\underline{\alpha}_l)(\underline{\alpha}_l - \tilde{\underline{x}}_l) + \sin(\tilde{\underline{x}}_l) = \sin(\underline{\alpha}_l), \quad (14)$$

which corresponds to a tangent point $t_l = \underline{\alpha}_l + 2k_l\pi$ at the original cycle of \underline{x} , and for any tangent point within the range of $[\underline{\alpha}_l + 2k_l\pi, 1.5\pi + 2k_l\pi]$, the tangent line is a valid lower bound. Similarly, we also consider the tangent line passing $(\bar{x}, \sin(\bar{x}))$, and we take $\tilde{\bar{x}}_l = \bar{x} - 2\bar{k}_l\pi$, where $\bar{k}_l = \lfloor \frac{\bar{x} - 1.5\pi}{2\pi} \rfloor$, so that $\tilde{\bar{x}}_l$ is within range $[1.5\pi, 3.5\pi]$. We also conduct a binary search to find the tangent point $\bar{\alpha}_l$, which corresponds to $\bar{\alpha}_l + 2\bar{k}_l\pi$ in the original cycle of \bar{x} , and for any tangent point within the range $[1.5\pi + 2\bar{k}_l\pi, \bar{\alpha}_l + 2\bar{k}_l\pi]$, the tangent line is also a valid lower bound. We make the tangent point optimizable with a parameter α_l ($\underline{\alpha}_l \leq \alpha_l \leq \bar{\alpha}_l$), which corresponds to a tangent line at tangent point t_l as the lower bound in Eq. (13) and Figure 5:

$$\begin{cases} a = \sin'(t_l) \\ b = \sin(t_l) - at_l \end{cases}, \quad (15)$$

$$\text{where } \begin{cases} t_l = \alpha_l + 2k_l\pi & \text{if } \underline{\alpha}_l \leq \alpha_l \leq 1.5\pi \\ t_l = \alpha_l + 2\bar{k}_l\pi & \text{if } 1.5\pi < \alpha_l \leq \bar{\alpha}_l \end{cases}. \quad (16)$$

In particular, when $\alpha_l = 1.5\pi$, both $\alpha_l + 2k_l\pi$ and $\alpha_l + 2\bar{k}_l\pi$ are tangent points for the same tangent line.



(a) The lower bound of Sin activation when $\alpha_l = \underline{\alpha}_l$.

(b) The lower bound of Sin activation when $\alpha_l = 1.5\pi$.

(c) The lower bound of Sin activation when $\alpha_l = \bar{\alpha}_l$.

Figure 5: Optimizing the lower bound of a Sin activation, where “Optimization range” shows all the valid tangent points for the lower bound during the optimization.

The derivation for the upper bound is similar. We take $\tilde{\underline{x}}_u = \underline{x} - 2k_u\pi$, where $k_u = \lfloor \frac{\underline{x} - 0.5\pi}{2\pi} \rfloor$, so that $\tilde{\underline{x}}_u$ is in range $[0.5\pi, 2.5\pi]$. And we take $\tilde{\bar{x}}_u = \bar{x} - 2\bar{k}_u\pi$, where $\bar{k}_u = \lfloor \frac{\bar{x} - 2.5\pi}{2\pi} \rfloor$, so that $\tilde{\bar{x}}_u$ is in range $[2.5\pi, 4.5\pi]$. Let $\underline{\alpha}_u$ be the tangent point where the tangent line crosses $\tilde{\underline{x}}_u$, and $\bar{\alpha}_u$ be the tangent point where the tangent line crosses $\tilde{\bar{x}}_u$, as found by a binary search. We define an optimizable parameter α_u ($\underline{\alpha}_u \leq \alpha_u \leq \bar{\alpha}_u$) which corresponds to a tangent line as the

upper bound:

$$\begin{cases} \bar{a} = \sin'(t_u) \\ \bar{b} = \sin(t_u) - \bar{a}t_u \end{cases}, \quad (17)$$

$$\text{where } \begin{cases} t_u = \alpha_u + 2k_u\pi & \text{if } \underline{\alpha}_u \leq \alpha_u \leq 2.5\pi \\ t_u = \alpha_u + 2\bar{k}_u\pi & \text{if } 2.5\pi < \alpha_u \leq \bar{\alpha}_u \end{cases}. \quad (18)$$

A.3 Optimizable Linear Relaxation for GeLU

For GeLU function where $x \in [\underline{x}, \bar{x}]$ are the intermediate bounds for x , we aim to relax and bound $\text{GeLU}(x)$ as:

$$\forall x \in [\underline{x}, \bar{x}], \quad \underline{a}x + \underline{b} \leq \text{GeLU}(x) \leq \bar{a}x + \bar{b}, \quad (19)$$

where $\underline{a}, \underline{b}, \bar{a}, \bar{b}$ are parameters in the linear bounds.

Given input range $[\underline{x}, \bar{x}]$, if $\bar{x} \leq 0$ or $\underline{x} \geq 0$, the range contains only one inflection point, the tangent point can be optimized in a way similar to bounding an S-shaped activation (Lyu et al., 2020). In other cases, $\underline{x} < 0$ and $\bar{x} > 0$ holds. For the upper bound, we use the line passing $(\underline{x}, \text{GeLU}(\underline{x}))$ and $(\bar{x}, \text{GeLU}(\bar{x}))$. For the lower bound, we derive two sets of tangent lines that crosses $(\underline{x}, \text{GeLU}(\underline{x}))$ and $(\bar{x}, \text{GeLU}(\bar{x}))$ with tangent points denoted as $\underline{\alpha}$ and $\bar{\alpha}$ respectively. We determine $\underline{\alpha}, \bar{\alpha}$ using a binary search that solves:

$$\begin{cases} \text{GeLU}'(\underline{\alpha})(\underline{\alpha} - \underline{x}) + \text{GeLU}(\underline{x}) = \text{GeLU}(\underline{\alpha}) \\ \text{GeLU}'(\bar{\alpha})(\bar{\alpha} - \bar{x}) + \text{GeLU}(\bar{x}) = \text{GeLU}(\bar{\alpha}) \end{cases}. \quad (20)$$

Any tangent line with a tangent point α ($\underline{\alpha} \leq \alpha \leq \bar{\alpha}$) is a valid lower bound, which corresponds to the lower bound in Eq. (19) with:

$$\begin{cases} \underline{a} = \text{GeLU}'(\alpha) \\ \underline{b} = \text{GeLU}(\alpha) - \alpha \text{GeLU}'(\alpha) \end{cases} \quad \text{s.t. } \underline{\alpha} \leq \alpha \leq \bar{\alpha}. \quad (21)$$

B Additional Results

B.1 Experiments on Self-Attention Networks from Wei et al. (2023)

To compare with Wei et al. (2023) that only supports verifying single-layer self-attention networks but not the entire ViT, we adopt pre-trained models from Wei et al. (2023) and run our verification methods under their settings, with 500 test images in MNIST using $\epsilon = 0.02$. We show the results in Table 5, where our methods also outperform Wei et al. (2023) on all the models.

Table 5: Number of verified instances out of 500 instances in MNIST with $\epsilon = 0.02$. A-small, A-medium and A-big are three self-attention networks with different parameter sizes from Wei et al. (2023).

Method	A-small	A-medium	A-big
Wei et al. (2023)	406	358	206
α, β -CROWN w/o BaB	444	388	176
GenBaB (ours)	450	455	232
Upper bound	463	479	482

B.2 Experiments on a ReLU Network

In this section, we study the effect of our BBPS heuristic on ReLU models. We adopt settings in Singh et al. (2019a,b); Müller et al. (2022) and experiment on a ‘‘ConvSmall’’ model with ReLU activation. The verification is evaluated on 1000 instances on CIFAR-10, following prior works. We show the results in Table 6, We find that on this ReLU network, our BBPS also works better than the BaBSR heuristic, when there is no *backup score* (46.0% verified by BBPS v.s. 45.6% verified by BaBSR). However, we find that recent works typically add a *backup score* for BaBSR, which is another heuristic score that serves as a backup for neurons with extremely small BaBSR scores. The backup score did not exist in the original BaBSR heuristic (Bunel et al., 2020) but it appeared in De Palma et al. (2021) and has also been

Table 6: Results on a ‘‘ConvSmall’’ model with ReLU activation (Singh et al., 2019a,b; Mller et al., 2022) on 1000 instances from CIFAR-10. Percentage of instances verified by various methods are reported. For methods other than PRIMA, we use α,β -CROWN as the underlying verifier but vary the branching heuristic. See explanation about the backup score in Appendix B.2.

Method	Verified
PRIMA	44.6%
BaBSR w/o backup score	45.6%
BaBSR w/ backup score	46.2%
Backup score only	45.0%
BBPS w/o backup score	46.0%
BBPS w/ backup score	46.2%

adopted by works such as Wang et al. (2021) when using BaBSR for ReLU networks. This backup score basically uses the intercept of the linear relaxation for the upper bound of a ReLU neuron that needs branching. Unlike BaBSR or BBPS, the backup score does not aim to directly estimate the change on the bounds computed by bound propagation, but aims to use the intercept to reflect the reduction of the linear relaxation after the branching. When the backup score is combined with BaBSR or BBPS for ReLU networks, the backup score seems to dominate the performance, where both BaBSR and BBPS have similar performance with the backup score added (46.2% verified), which hides the underlying improvement of BBPS over BaBSR by providing a more precise estimation. However, the backup score is specifically for ReLU, assuming that the intercept of the linear relaxation can reflect the reduction of the linear relaxation, which is not the case for general nonlinearities. We leave it for future work to study the possibility of designing a backup score for general nonlinearities.

C Experimental Details

Verification. We implement our verification algorithm based on auto_LiRPA³ and α,β -CROWN⁴. Our BaB is batched where multiple domains are branched in parallel, and the batch size is dynamic tuned based on the model size to fit the GPU memory. To pre-optimize the branching points, we enumerate the branching points (p in Eq. (6)) with a step size instead of performing gradient descent, considering that we only have up to two parameters for the branching points in our experiments. For nonlinearities with a single input, we use a step size of 0.01, and for nonlinearities with two inputs, we use a step size of 0.1. We pre-optimize the branching points for intermediate bounds within the range of $[-5, 5]$. For all the experiments, each experiment is conducted using a single NVIDIA GTX 1080Ti GPU.

Training the models. To train our models on CIFAR-10, we use PGD adversarial training (Madry et al., 2018). We use 7 PGD steps during the training and the step size is set to $\epsilon/4$. For training the Sigmoid networks in Table 3, we use the SGD optimizer with a learning rate of 5×10^{-2} for 100 epochs; and for training the Tanh networks, we use the SGD optimizer with a learning rate of 1×10^{-2} for 100 epochs. For training the LSTMs in Table 4, we use the Adam optimizer with a learning of 10^{-3} for 30 epochs. And for training the ViTs, we use the Adam optimizer with a learning of 5×10^{-3} for 100 epochs. For Sine networks, we use the SGD optimizer with a learning rate of 1×10^{-3} for 100 epochs

³https://github.com/Verified-Intelligence/auto_LiRPA

⁴<https://github.com/Verified-Intelligence/alpha-beta-CROWN>